

**Pressure-induced electronic spin transition of iron in magnesiowustite-(Mg,Fe)O**Jung-Fu Lin,<sup>1</sup> Alexander G. Gavriluk,<sup>2,3,4</sup> Viktor V. Struzhkin,<sup>2</sup> Steven D. Jacobsen,<sup>2</sup> Wolfgang Sturhahn,<sup>5</sup> Michael Y. Hu,<sup>6</sup> Paul Chow,<sup>6</sup> and Choong-Shik Yoo<sup>1</sup><sup>1</sup>*Lawrence Livermore National Laboratory, 7000 East Avenue, Livermore, California 94550, USA*<sup>2</sup>*Geophysical Laboratory, Carnegie Institution of Washington, 5251 Broad Branch Road NW, Washington, DC 20015, USA*<sup>3</sup>*Institute for High-Pressure Physics, Troitsk, Moscow oblast, 142190 Russia*<sup>4</sup>*Institute of Crystallography, Russian Academy of Sciences, 117333, Leninskii prospekt 59, Moscow, Russia*<sup>5</sup>*Advanced Photon Source, Argonne National Laboratory, 9700 South Cass Avenue, Argonne, Illinois 60439, USA*<sup>6</sup>*HPCAT, Advanced Photon Source, Argonne National Laboratory, 9700 South Cass Avenue, Argonne, Illinois 60439, USA*

(Received 30 January 2006; published 15 March 2006)

An electronic transition of iron in magnesiowustite has been studied with synchrotron Mössbauer and x-ray emission spectroscopies under high pressures. Synchrotron Mössbauer studies show that the quadrupole splitting disappears and the isomer shift drops significantly across the spin-pairing transition of iron in (Mg<sub>0.75</sub>,Fe<sub>0.25</sub>)O between 52 and 70 GPa. Based upon current results and percolation theory, we reexamine the high-pressure phase diagram of (Mg,Fe)O and find that iron-iron exchange interaction plays an important role in stabilizing the high-spin state of iron in FeO-rich (Mg,Fe)O.

DOI: [10.1103/PhysRevB.73.113107](https://doi.org/10.1103/PhysRevB.73.113107)

PACS number(s): 71.30.+h, 71.20.Be, 71.27.+a

Magnesiowustite [(Mg,Fe)O] with the cubic rock-salt (B1) structure forms a solid solution between periclase (MgO) and wustite (Fe<sub>1-x</sub>O).<sup>1-9</sup> Periclase is a wide band gap insulator and prototype simple monoxide, whereas wustite, a classical Mott insulator, is an important member of the highly correlated transition metal monoxide (TMO) group including NiO, CoO, and MnO.<sup>10-18</sup> The Mott insulator-metal transition results from the closure of the Mott-Hubbard *d-d* band gap or of the charge-transfer *p-d* gap, and the strength of electron correlation in the TMO systems is characterized by the ratio between the on-site *d-d* Coulomb interaction energy (*U*) and *3d* bandwidth (*W*).<sup>10</sup> In TMO compounds, a high-spin to low-spin (spin-pairing) transition occurs when the crystal field splitting exceeds the Hund's-rule exchange energy and the material becomes diamagnetic, resulting in the collapse of magnetic state.<sup>10</sup> Although Mott insulator-metal transitions in TMO have been predicted to occur under high pressures,<sup>10,12</sup> it is only very recently that such transition has been experimentally observed in MnO.<sup>15,17</sup> On the other hand, high-pressure x-ray emission spectroscopy (XES) studies indicated that FeO remains a magnetic insulator up to at least 143 GPa.<sup>13,14</sup> (Mg,Fe)O contains partially occupied Fe<sup>2+</sup> in *3d* orbitals situated in the band gap.<sup>1,2,9</sup> Hence the local environment of iron, the *3d* bandwidth, and iron-iron interaction play an important role in the electronic, structural, and physical properties of magnesiowustite under high pressures. Studies of the complete solid solution MgO-FeO system should thus shed light on the questions regarding the magnetic collapse in highly correlated TMO systems such as FeO at high pressure.

Pressure-induced electronic spin transitions of iron have been described theoretically<sup>1,2,9</sup> and experimentally reported to occur in MgO-rich magnesiowustite based on high-pressure XES observation of the Fe-K $\beta$  fluorescence lines in the sample.<sup>5,8</sup> Since magnesiowustite is the second most abundant mineral in the Earth's lower mantle, the electronic spin transition of iron in magnesiowustite in the Earth's lower mantle may have major geophysical and geochemical

consequences.<sup>1,2,5,8,9</sup> However, recent traditional Mössbauer studies suggested that high-spin and low-spin states of iron could coexist in magnesiowustite over a very wide range of pressures, leading to a spin crossover at high pressures.<sup>19,20</sup> The apparent discrepancy has led us to investigate the magnetic states of the system using both synchrotron Mössbauer spectroscopy (SMS)<sup>21</sup> and XES under high pressures. SMS spectra, for Fe<sup>2+</sup> systems in particular, offer a direct way of obtaining the relative concentrations of the spin states since each is associated with its own characteristic set of Mössbauer spectral parameters, isomer shift (IS), and quadrupole splitting (QS).<sup>22</sup> Based on previous traditional Mössbauer studies on oxides and silicates under ambient conditions, a decrease in IS and the significant decrease or absence of the QS are expected for the transition from the high-spin state to the low-spin state.<sup>3,22,23</sup>

A polycrystalline <sup>57</sup>Fe-enriched (Mg<sub>0.75</sub>,Fe<sub>0.25</sub>)O sample was synthesized by sintering stoichiometric mixtures of MgO and <sup>57</sup>Fe (>95% enrichment) powder at 1378–1478 K for 8 h under a controlled CO<sub>2</sub>-CO atmosphere near the iron-wustite buffer.<sup>3</sup> After three cycles of grinding and sintering, the final product was compositionally homogeneous in electron microprobe analyses and its ferric iron (Fe<sup>3+</sup>) content was below the detection limit of Mössbauer spectroscopy. X-ray diffraction data showed that the sample was in the B1 structure with a cell parameter of 4.2411 ( $\pm 0.0004$ ) Å,<sup>4</sup> and magnetite (Fe<sub>3</sub>O<sub>4</sub>) was not detected. To prevent the effects of a large sample thickness on the SMS data (a thinner sample provides less distortion to the shape of the SMS spectra) and to reduce potential pressure gradient in the sample in the axial direction of the sample chamber, the sample was flattened down between two flat diamonds (5  $\mu$ m in thickness in Run #1 and 1  $\mu$ m in thickness in Run #2); the effective thickness, a parameter to describe the total intensity and the influence of the sample thickness on the shape of the SMS spectra in this composition, was estimated to be between two and three.<sup>21</sup> Such sample preparation also ensured the homogeneous thickness of the sample. A rhenium gasket was pre-

indented to a thickness of 20  $\mu\text{m}$  and a hole of 80  $\mu\text{m}$  was drilled in it. A small flake of the sample with  $\sim 60 \mu\text{m}$  in diameter was loaded into the sample chamber of a diamond anvil cell (DAC) with flat diamonds of a culet size of 200  $\mu\text{m}$ . Subsequently, KCl was loaded into the sample chamber as the pressure medium and a few small ruby balls were placed close to the sample for pressure measurements using the ruby  $R_1$  luminescence peak.<sup>24</sup>

SMS experiments were carried out at the undulator beamline 3-IDB and 16-IDD of the Advanced Photon Source (APS), Argonne National Laboratory (ANL).<sup>21</sup> A monochromatic x-ray beam of  $\sim 14.4125 \text{ keV}$  with 1 meV resolution at 3-ID and 2 meV resolution at 16-IDD was used to excite the nuclear resonance of the  $^{57}\text{Fe}$  nuclei in the sample. The focused x-ray beam was approximately 7  $\mu\text{m}$  in diameter at 3-IDB and 20  $\mu\text{m}$  in diameter at 16-IDD, where a cleanup slit of 20  $\mu\text{m}$  in diameter was used to get rid of unwanted tail of the focused x-ray beam. The very small x-ray beam-size significantly reduced the influence of the pressure gradients in the radial direction across the sample chamber. The time delayed spectra were recorded by an avalanche photodiode detector in the forward direction. After the SMS spectrum of the sample had been collected, thin stainless steel foil ( $\text{Fe}_{55}\text{Cr}_{20}\text{Ni}_{25}$ ) of 1.4  $\mu\text{m}$  (Run #1) or 0.5  $\mu\text{m}$  (Run #2) in thickness was placed outside of the DAC to serve as a reference for the IS measurements.<sup>21–23</sup> The data collection time for each SMS spectrum was between 1 and 4 h. The SMS spectra were evaluated with the MOTIF<sup>25</sup> and CONUSS<sup>21</sup> programs to derive the hyperfine parameters, QS and IS.

SMS spectra of the sample only and of the sample with stainless steel reference were collected up to 92 GPa at 300 K (Fig. 1). The derived QS and IS parameters under ambient conditions are consistent with high-spin  $\text{Fe}^{2+}$  in octahedral coordination in oxides and silicates (Fig. 2).<sup>3,22,23</sup> The QS increases with increasing pressure up to about 30 GPa, plateaus at further pressure increase to about 60 GPa, and disappears at above 70 GPa. The IS of the high-spin state decreases with increasing pressure and a noticeable drop of the IS occurs at approximately 63 GPa. The simultaneous disappearance of the QS and the drop of the IS at about 63 GPa are consistent with a high-spin to low-spin electronic transition of iron in the sample between 52 and 70 GPa,<sup>5,8</sup> although the width of the transition remains to be further investigated. Based on the modeling of the SMS spectra, the ratio of the high-spin to low-spin states of iron in  $(\text{Mg}_{0.75}, \text{Fe}_{0.25})\text{O}$  as a function of pressure are also consistent with the changes in the QS and IS. The QS arises from the interaction between the nuclear quadrupole moment and the nonspherical component of the electronic charge distribution described by its effective electric-field gradient ( $\Delta$ ) in a simplified model. In general, the electric-field gradient in the vicinity of the  $^{57}\text{Fe}$  nucleus can be attributed to a lattice contribution from the crystal field produced by the surrounding ions ( $\Delta_{\text{lat}}$ ) and an electronic contribution from the nonspherical charge distribution of the electron shell surrounding the nucleus ( $\Delta_{\text{el}}$ ).<sup>22</sup> Since the electronic spin transition of iron in ferroperricite is isosymmetric with a very small volume decrease from x-ray diffraction studies,<sup>8</sup> a significant change in the  $\Delta_{\text{lat}}$  is not expected across the transition.

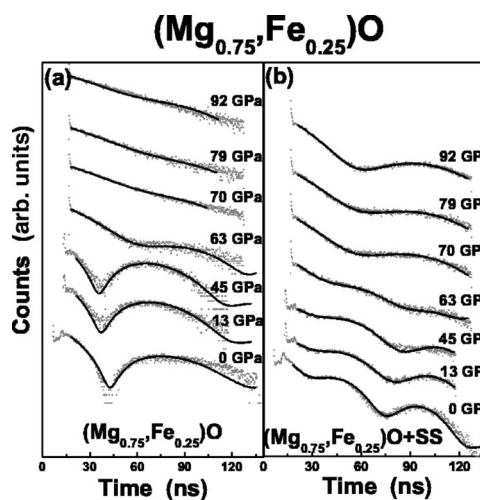


FIG. 1. Representative SMS spectra of (a)  $(\text{Mg}_{0.75}, \text{Fe}_{0.25})\text{O}$  and (b)  $(\text{Mg}_{0.75}, \text{Fe}_{0.25})\text{O}$  with stainless steel (SS) as a function of pressure at room temperature. Black line, modeled spectrum with the MOTIF program (Ref. 25). The sample thickness was approximately 1  $\mu\text{m}$ , and the thickness of the stainless steel foil was about 0.5  $\mu\text{m}$ . Evolution of the SMS spectra of  $(\text{Mg}_{0.75}, \text{Fe}_{0.25})\text{O}$  with the stainless steel as a reference enables derivation of the IS of the sample as a function of pressure (see Fig. 2). The quantum bits at 0, 13, and 45 GPa are generated from the QS of the high-spin state of iron in the sample, whereas the flat feature of the spectra at 70, 79, and 92 GPa indicates disappearance of the QS.

Therefore  $\Delta_{\text{el}}$  is most likely the main contribution to the sudden change of the QS and the significant decrease in the IS at about 63 GPa. That is, the effective electric field gradient is dramatically reduced due to the spin-pairing transition; the electron shell of  $\text{Fe}^{2+}$  ions in the octahedral coordination of the high-spin state is spherically asymmetric with  $S=2$  and  $t_{2g}^3 e_g^2 t_{2g}^1$  (only two electrons are paired and four are unpaired) and  $\text{Fe}^{2+}$  ions in the low-spin state are more spherically symmetric with  $S=0$  and  $t_{2g}^3 t_{2g}^3$  (all six electrons are paired).

Furthermore, the IS is proportional to the difference in the nuclear radii between the ground and excited states and the electron density at the nucleus (also called the contact density).<sup>22</sup> The electron density at the nucleus consists of the  $s$ -electron density at the nucleus including the perturbing effect of the outer electrons. Therefore the negative slope in IS as a function of pressure reflects the increase in density with pressure in the high-spin state and low-spin state, respectively, whereas the spin-pairing process in the  $3d$  electrons causes a jump in the total  $s$ -electron density at the nucleus and hence a drop in the IS. The magnitude of the change in the IS across the electronic spin-pairing transition of iron in magnesio-wustite at approximately 63 GPa is, in general, consistent with that observed in other iron oxides and silicates under ambient conditions.<sup>26</sup> The  $d(\text{IS})/dP$  for the low-spin state is lower than that of the high-spin state, suggesting an increase in the incompressibility across the transition [Fig. 2(b)]. It has been observed in x-ray diffraction experiments that the high-spin to low-spin transition of iron in magnesio-wustite results in a much higher bulk modulus ( $K_T$ ) and bulk sound velocity ( $V_\phi$ ) for the high-pressure low-spin state;  $K_T$

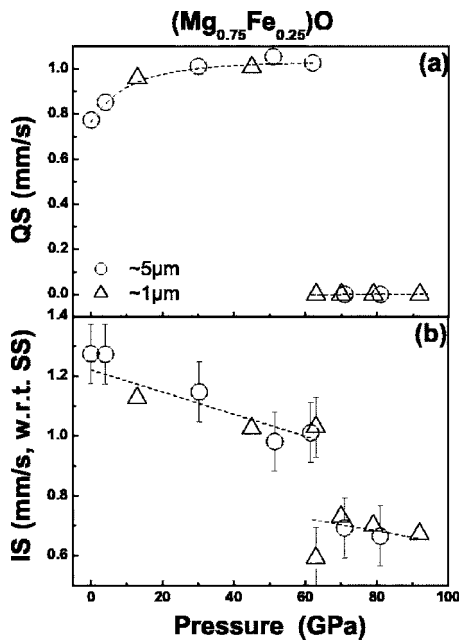


FIG. 2. Pressure dependence of (a) QS and (b) IS (with respect to stainless steel standard) in  $(\text{Mg}_{0.75}, \text{Fe}_{0.25})\text{O}$  as revealed from the modeling of the SMS spectra. Open triangle: this study from sample of  $\sim 1 \mu\text{m}$  in thickness and SS of  $\sim 0.5 \mu\text{m}$  (Run #2); open circles: this study from sample of  $\sim 5 \mu\text{m}$  and SS of  $\sim 1.4 \mu\text{m}$  (Run #1); vertical bars: error bars for the IS and QS. The error bars for the IS in Run #2 (except at 63 GPa) and for the QS are smaller than the symbol; the relatively larger errors in the IS in Run #1 were due to the dynamic effects (larger sample thickness). The pressure uncertainty ( $1\sigma$ ) estimated from multiple pressure measurements of the ruby luminescence lines was typically 3%–5%. A least-squares fit to the IS (short dash lines) gives  $d(\text{IS})/dP$  of  $-0.0037(\pm 0.0007)$  mm/s GPa for the high-spin state and  $d(\text{IS})/dP$  of  $-0.0021(\pm 0.0010)$  mm/s GPa for the low-spin state, respectively. The spectrum at 63 GPa is modeled with two states, a low-spin state of  $\text{Fe}^{2+}$  (20% in ratio) with no QS and a state with a QS of  $0.56(\pm 0.10)$  mm/s. The nature of the intermediate state remains to be further investigated in the future.

jumps by  $\sim 35\%$  and  $V_{\Phi}$  increases by  $\sim 15\%$  across the transition in  $(\text{Mg}_{0.83}, \text{Fe}_{0.17})\text{O}$ .<sup>8</sup>

To understand the compositional effect on the spin transition in the system, we also carried out *in situ* XES experiments on  $(\text{Mg}_{0.95}, \text{Fe}_{0.05})\text{O}$  in a DAC. XES spectra of the Fe- $K\beta$  fluorescence lines in dilute  $(\text{Mg}_{0.95}, \text{Fe}_{0.05})\text{O}$  showed that a high-spin to low-spin transition occurs between 46 and 55 GPa (Fig. 3). In light of the observed electronic transition in magnesiowustite at high pressures and room temperature, we reexamined the high-pressure phase diagram of the MgO-FeO system (Fig. 3). Based on high-pressure x-ray diffraction, XES, and SMS studies, a B1-rhombohedral structural transition occurs in the FeO-rich region and addition of MgO stabilizes the B1 structure to much higher pressures,<sup>6,7</sup> whereas an isosymmetric electronic transition from the paramagnetic state (PM) to the diamagnetic state (DM) occurs in the MgO-rich region and addition of FeO into MgO stabilizes the high-spin state to much higher pressures.<sup>5,8</sup> The isosymmetric electronic transition may terminate at a critical point of temperature.<sup>9</sup>

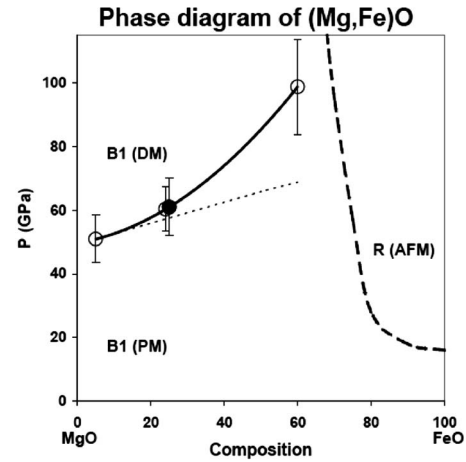


FIG. 3. Phase diagram of the magnesiowustite- $(\text{Mg}, \text{Fe})\text{O}$  system under high pressures and room temperature. Open circle, XES results (Ref. 8); closed circle, SMS results. An isosymmetric transition from the paramagnetic state (PM) to the diamagnetic state (DM) occurs in MgO-rich magnesiowustite (ferropericlase) (Refs. 5 and 8), and addition of FeO in MgO stabilizes the high-spin state to much higher pressures (Ref. 8). On the other hand, addition of MgO in FeO stabilizes the B1 structure relative to the antiferromagnetic (AFM) rhomboheral phase (R) to much higher pressures (Ref. 6). Potential electronic and structural transitions in the FeO-rich region remain to be further understood. The dotted line represents the calculated high-spin to low-spin transition boundary based on the assumption that the spin transition occurs at the same Fe–O bond length and the iron-iron exchange interaction could be neglected.

Here we further assess the effect of iron-iron exchange interaction on the electronic transition using percolation theory.<sup>27</sup> If one neglects the iron-iron exchange interactions between neighboring iron atoms in the system (i.e., at very low iron concentration in the system), the slope of the electronic spin transition as a function of FeO concentration ( $x$ ) can be evaluated from the lattice expansion due to the substitution of the  $\text{Mg}^{2+}$  ions with the larger  $\text{Fe}^{2+}$  which creates an internal pressure on the local  $\text{Fe}^{2+}$  ions in addition to the external pressure in a DAC. The transition pressure as a function of FeO concentration ( $dP/dx$ ) can thus be calculated from the assumption that the spin transition occurs at the same Fe–O bond length; the same internal pressure. Since the addition of 50 at % of FeO into MgO expands the MgO lattice by approximately 1.4%,<sup>4</sup> an additional pressure of about 15 GPa is needed to reach the electronic transition in  $(\text{Mg}_{0.50}, \text{Fe}_{0.50})\text{O}$  (Fig. 3). However, it is clear from Fig. 3 that the spin-paring transition observed experimentally in the FeO-rich region occurs at much higher pressure than what the simple calculation predicted. This discrepancy occurs due to the contribution of the Fe-Fe exchange interaction which further stabilizes the high-spin state to much higher pressures. Based on percolation theory, for the face-centered-cubic (fcc) lattice the random impurity has a percolation threshold, a continuous percolation path through the three-dimensional fcc structure, at about 12% concentration.<sup>27</sup> When iron concentration in the  $(\text{Mg}, \text{Fe})\text{O}$  system is above the percolation threshold,  $\text{Fe}^{2+}$  atoms form an infinitely connected percolation path through the whole structure, where

each  $\text{Fe}^{2+}$  atom has at least two  $\text{Fe}^{2+}$  neighbors. That is, the  $3d$  outer electrons of an  $\text{Fe}^{2+}$  atom interact with the neighboring  $3d$  electrons of the  $d_{xy}$ ,  $d_{xz}$ , and  $d_{zy}$  orbitals, which correspond to the  $t_{2g}$  states (split down from the  $e_{2g}$  orbitals by the octahedral crystal field). This iron-iron interaction would increase the effective crystal field by further splitting mostly  $t_{2g}$  orbitals and lowering them with respect to the  $e_{2g}$  orbitals and thus would stabilize the high-spin state in the system. In particular, the FeO end member of the magnesio-wustite system is well-known for its strength of electron correlation which is characterized by the ratio between the on-site  $d$ - $d$  Coulomb interaction energy ( $U$ ) and  $3d$  bandwidth ( $W$ ).<sup>10</sup> Based on the extrapolated electronic transition boundary from our studies, the high-spin to low-spin transition may occur at a pressure above 160 GPa, though the effects of the B1-rhombohedral and the B1-NiAs (or anti-NiAs) structural transition in the very FeO-rich end on the electronic transition should be further considered; the potential magnetic collapse and metallization in FeO under high pressures is suggested to be associated with a structural phase transformation to NiAs or anti-NiAs.<sup>11,28</sup>

In summary, we have studied the pressure-induced electronic spin transition in magnesio-wustite by high-pressure SMS and XES. Our SMS studies of  $(\text{Mg}_{0.75}, \text{Fe}_{0.25})\text{O}$  have shown the disappearance of the quadrupole splitting and the significant drop of the isomer shift between 52 and 70 GPa, consistent with a high-spin to low-spin transition of iron in

the sample. Based on current results and percolation theory, we reexamined the high-pressure phase diagram of the MgO-FeO system and found that iron-iron exchange interaction in the system plays an important role in stabilizing the high-spin state of iron in the FeO-rich region of the system. Our results indicate that the same iron-iron correlation effect is also responsible for stabilizing of the high-spin of iron in FeO to much higher pressures and the magnetic collapse in FeO may occur at a pressure above 160 GPa.

We acknowledge HPCAT and XOR-3, APS, ANL for the use of the synchrotron facilities. We thank H.C. Cynn, I. Lyubutin, V. Iota, J.M. Jackson, J. Tse, A. McMahan, and P. Soderlind for helpful discussions, J. Kung for the  $(\text{Mg}_{0.95}, \text{Fe}_{0.05})\text{O}$  sample, and J. Zhao, M. Lerche, and E. Rod for their assistance in SMS experiments. This work and use of the APS are supported by U.S. DOE, Basic Energy Sciences, Office of Science, under Contract No. W-31-109-ENG-38, and the State of Illinois under HECA. This work at LLNL was performed under the auspices of the U.S. DOE by University of California and LLNL under Contract No. W-7405-Eng-48. A.G.G. was supported by Russian Foundation for Basic Research Grants No. 04-02-16945a and No. 05-02-16142a, and by the Program of Physical Branch of the Russian Academy of Sciences under the project of "Strong Correlating Electron Systems." V.V.S. acknowledges financial support from DOE and S.D.J. acknowledges financial support from NSF-EAR 0440112.

- <sup>1</sup>D. M. Sherman, *J. Geophys. Res.* **96**, 14299 (1991).
- <sup>2</sup>D. M. Sherman and H. J. F. Jansen, *Geophys. Res. Lett.* **22**, 1001 (1995).
- <sup>3</sup>D. P. Dobson, N. S. Cohen, Q. A. Pankhurst, and J. P. Brodholt, *Am. Mineral.* **83**, 794 (1998).
- <sup>4</sup>S. D. Jacobsen, H. J. Reichmann, H. Spetzler, S. J. Mackwell, J. R. Smyth, R. J. Angel, and C. A. McCammon, *J. Geophys. Res.* **107**, 2037 (2002).
- <sup>5</sup>J. Badro, G. Fiquet, F. Guyot, J. P. Rueff, V. V. Struzhkin, G. Vankó, and G. Monaco, *Science* **300**, 789 (2003).
- <sup>6</sup>J. F. Lin, D. L. Heinz, H. K. Mao, R. Hemley, J. M. Devine, J. Li, and G. Shen, *Proc. Natl. Acad. Sci. U.S.A.* **100**, 4405 (2003).
- <sup>7</sup>S. D. Jacobsen, H. Spetzler, H. J. Reichmann, and J. R. Smyth, *Proc. Natl. Acad. Sci. U.S.A.* **100**, 5867 (2004).
- <sup>8</sup>J. F. Lin, V. V. Struzhkin, S. D. Jacobsen, M. Hu, P. Chow, J. Kung, H. Liu, H. K. Mao, and R. J. Hemley, *Nature (London)* **436**, 377 (2005).
- <sup>9</sup>W. Sturhahn, J. M. Jackson, and J. F. Lin, *Geophys. Res. Lett.* **32**, L12307 (2005).
- <sup>10</sup>M. F. Mott, *Metal Insulator Transitions* (Taylor and Francis, London, 1990).
- <sup>11</sup>Y. Fei and H. K. Mao, *Science* **266**, 1678 (1994).
- <sup>12</sup>R. E. Cohen, I. I. Mazin, and D. G. Isaak, *Science* **275**, 654 (1997).
- <sup>13</sup>M. P. Pasternak, R. D. Taylor, R. Jeanloz, X. Li, J. H. Nguyen, and C. A. McCammon, *Phys. Rev. Lett.* **79**, 5046 (1997).
- <sup>14</sup>J. Badro, V. V. Struzhkin, J. Shu, R. J. Hemley, H. K. Mao, C. C. Kao, J. P. Rueff, and G. Shen, *Phys. Rev. Lett.* **83**, 4101 (1999).
- <sup>15</sup>J. R. Patterson, C. M. Aracne, D. D. Jackson, V. Malba, S. T. Weir, P. A. Baker, and Y. K. Vohra, *Phys. Rev. B* **69**, 220101(R) (2005).
- <sup>16</sup>J. P. Rueff, A. Mattila, J. Badro, G. Vanko, and A. Shukla, *J. Phys.: Condens. Matter* **17**, S717 (2005).
- <sup>17</sup>C. S. Yoo, B. Maddox, J.-H. P. Klepeis, V. Iota, W. Evans, A. McMahan, M. Y. Hu, P. Chow, M. Somayazulu, D. Häusermann, R. T. Scalettar, and W. E. Pickett, *Phys. Rev. Lett.* **94**, 115502 (2005).
- <sup>18</sup>G. Peng, X. Wang, C. R. Randall, J. A. Moore, and S. P. Cramer, *Appl. Phys. Lett.* **65**, 2527 (1994).
- <sup>19</sup>I. Yu. Kantor, L. S. Dubrovinsky, and C. A. McCammon, *Joint 20th AIRAPT-43th EHPRG, Karlsruhe, Germany* (Forschungszentrum, Karlsruhe, 2005).
- <sup>20</sup>S. Speziale, A. Milner, V. E. Lee, S. M. Clark, M. P. Pasternak, and R. Jeanloz, Iron spin transition in Earth's mantle, *Proc. Natl. Acad. Sci. U.S.A.* **102**, 17918 (2005).
- <sup>21</sup>W. Sturhahn, *J. Phys.: Condens. Matter* **16**, S497 (2004).
- <sup>22</sup>A. G. Maddock, *Mössbauer Spectroscopy: Principles and Applications of the Techniques* (Horwood Publishing, Chichester, 1997).
- <sup>23</sup>G. Shirane, D. E. Cox, and S. L. Ruby, *Phys. Rev.* **125**, 1158 (1962).
- <sup>24</sup>H. K. Mao, P. M. Bell, J. W. Shaner, and D. J. Steinberg, *J. Appl. Phys.* **49**, 3276 (1978).
- <sup>25</sup>Yu. V. Shvyd'ko, *Phys. Rev. B* **59**, 9132 (1999).
- <sup>26</sup>F. C. Hawthorne, in *Spectroscopic Methods in Mineralogy and Geology*, edited by F. C. Hawthorne (BookCrafters, Michigan, 1988), pp. 255-333.
- <sup>27</sup>C. D. Lorenz and R. M. Ziff, *Phys. Rev. E* **57**, 230 (1998).
- <sup>28</sup>I. I. Mazin, Y. Fei, R. Downs, and R. Cohen, *Am. Mineral.* **83**, 451 (1998).